

Unusual X-ray excited luminescence spectra of NiO suggestive of a self-trapping of the $d-d$ charge transfer exciton

V.I. Sokolov,¹ V.A. Pustovarov,² V.N. Churmanov,² V.Yu. Ivanov,²
N.B. Gruzdev,¹ P.S. Sokolov,³ A.N. Baranov,³ and A.S. Moskvina⁴

¹*Institute of Metal Physics UD RAS, S. Kovalevskaya Str. 18, 620990, Ekaterinburg, Russia*

²*Ural Federal University, Mira Str., 19, 620002 Ekaterinburg, Russia*

³*Lomonosov Moscow State University, 119991, Moscow, Russia*

⁴*Department of Theoretical Physics, Institute of Natural Science,
Ural Federal University, Lenin Str., 51, 620083 Ekaterinburg, Russia*

(Dated: January 5, 2014)

Luminescence spectra of NiO have been investigated under vacuum ultraviolet (VUV) and soft X-ray (XUV) excitation. Photoluminescence (PL) spectra show broad emission bands centered at about 2.3 and 3.2 eV. The PL excitation (PLE) spectral evolution and lifetime measurements reveal that two mechanisms with short and long decay times, attributed to the $d(e_g)-d(e_g)$ and $p(\pi)-d$ charge transfer (CT) transitions in the range 4-6 eV, respectively, are responsible for the observed emissions, while the most intensive $p(\sigma)-d$ CT transition at 7 eV appears to be a weak if any PL excitation mechanism. The PLE spectra recorded in the 4-7 eV range agree with the RIXS and reflectance data. Making use of the XUV excitation allows us to avoid the predominant role of the surface effects in luminescence and reveal bulk luminescence with puzzling well isolated doublet of very narrow lines with close energies near 3.3 eV characteristic for recombination transitions in self-trapped $d-d$ CT excitons formed by coupled Jahn-Teller Ni^{2+} and Ni^{3+} centers. This conclusion is supported both by a comparative analysis of the luminescence spectra for NiO and solid solutions $Ni_xZn_{1-x}O$, and by a comprehensive cluster model assignment of different $p-d$ and $d-d$ CT transitions, their relaxation channels. To the best of our knowledge it is the first observation of the self-trapping for $d-d$ CT excitons. Our paper shows the time resolved luminescence measurements provide an instructive tool for elucidation of the $p-d$ and $d-d$ CT excitations and their relaxation in 3d oxides.

I. INTRODUCTION

Explaining the electronic properties of transition metal monoxides is one of the long-standing problems in the condensed matter physics. Nickel monoxide NiO with its rather simple rocksalt structure, a large insulating gap and an antiferromagnetic ordering temperature of $T_N = 523$ K has been attracting many physicists as a prototype oxide for this problem. This strongly correlated electron material has played and is playing a very important role in clarifying the electronic structure and understanding the rich physical properties of 3d compounds. Recent discoveries of a giant low frequency dielectric constant, bistable resistance switching, and other unconventional properties¹ have led to a major resurgence of interest in NiO.

However, despite several decades of studies² there is still no literature consensus on the detailed electronic structure of NiO. Different energy gap (E_g) values between 3.7 and 5 eV^{3,4} are reported for NiO and reliable E_g still remains to be settled. Conventional band theories which stress the delocalized nature of electrons cannot explain this large gap and predict NiO to be metallic. NiO has long been viewed as a prototype "Mott insulator",² with gap formed by intersite $d-d$ charge transfer (CT) transitions, however, this view was later replaced by that of a "CT insulator"⁵ with gap formed by $p-d$ CT transitions. Most recent RIXS and optical reflectivity measurements⁴ showed that the CT band peaked

near 4-5 eV reveals a discernible q -dispersion of its energy typical for Mott-Hubbard $d-d$ CT transitions while intensive CT band at higher energy peaked near 7-8 eV reveals only intensity dispersion without any visible dispersion of the energy that is typical for intra-center $p-d$ CT transitions. Nevertheless, to date we have no comprehensive assignment of different spectral features in NiO to $p-d$ or $d-d$ CT transitions.

Although the optical absorption of NiO have been studied experimentally with some detail, their optical emission properties have been scarcely investigated. However, luminescence spectroscopy can give a profound insight into the electronic structure, electron-hole excitations and their relaxation in the lattice. Different measurements performed with UV excitation below and near optical gap⁶⁻⁸ point to a broad luminescence band in the region 2-3.5 eV. The temperature behavior indicates that the broad PL spectra of NiO consist of several components with relative intensity dependent on the temperature and excitation energy. The low-energy excitation ($E_{exc} \approx 2.4$ eV) below the charge-transfer gap stimulates a photoemission in single-crystal NiO with two maxima, one at 1.5-1.6 eV and a larger one at 2.2-2.3 eV⁹. Green luminescence band with a maximum around 2.25 eV has been observed in nanoclustered NiO at $E_{exc} \leq 2.95$ eV⁷. The observed emission bands in the visible and near infrared spectral ranges are usually attributed to Ni^{2+} intrasite, or crystal field $d-d$ transitions. In particular, the main green luminescence band peaked near 2.3 eV is

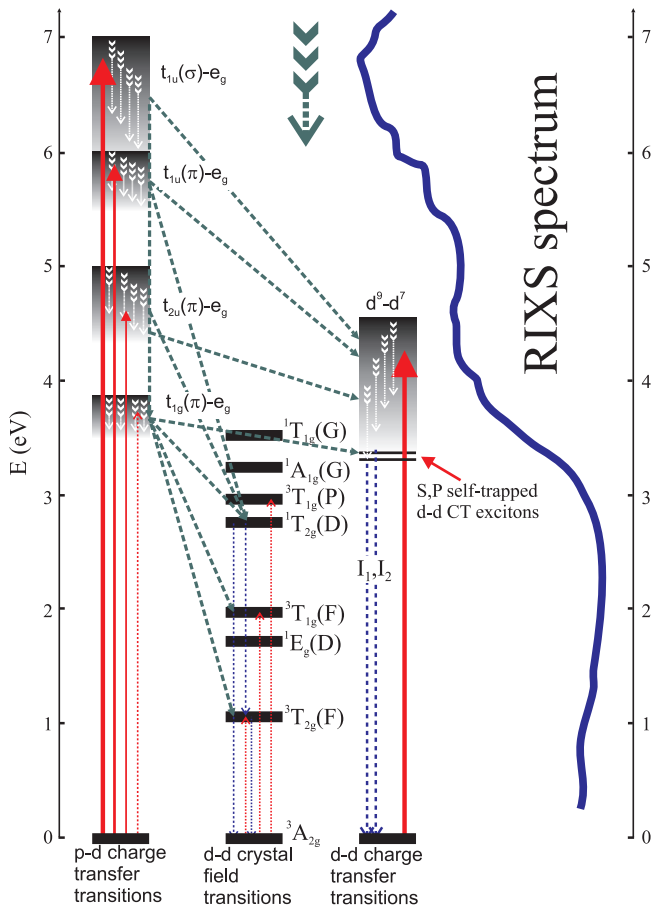


FIG. 1: (Color online) Spectra of the d - d , p - d CT transitions and intracenter crystal field d - d transitions in NiO. Strong dipole-allowed $\sigma - \sigma$ d - d and p - d transitions are shown by thick solid arrows; weak dipole-allowed $\pi - \sigma$ p - d transitions by thin solid arrows; weak dipole-forbidden low-energy transitions by thin dashed arrows, respectively. Dashed lines point to different EH relaxation channels, dotted lines point to PL transitions. Spectrum of the crystal field d - d transitions is reproduced from Ref. 10. Right hand side reproduces a fragment of the RIXS spectra for NiO¹⁵.

attributed to a Stokes-shifted ${}^1T_{2g}(D) \rightarrow {}^3A_{2g}(F)$ transition while the low-energy band peaked near 1.5 eV is related to ${}^1E_g(D) \rightarrow {}^3A_{2g}(F)$ transition⁹ (see Fig. 1 for the spectrum of the crystal field d - d transitions¹⁰). However, the photoluminescence spectra of bulk single crystals and ceramics of NiO under 3.81 eV photoexcitation⁸ suggestive the band gap excitation have revealed in addition to the green band a more intensive broad violet PL band with a maximum around 3 eV. The band was related to a p - d charge transfer. Radiative recombination of carriers in powdered pellets of NiO under UV excitation with $E_{exc} = 4.43$ eV (280 nm) higher than the CT gap consists at 10 K of a broad intensive band peaked at 2.8 eV with a shoulder centered at about 3.2 eV⁶. It is clearly appreciated that the 2.8 eV emission band decreases with increasing temperature, while the 3.2 eV band follows a strictly opposite trend and becomes the dominant emis-

sion at about 150 K. Furthermore, the 3.2 eV band reveals a two-peak structure clearly visible at elevated temperatures. Different kinetic properties, seemingly different temperature behavior⁶ point to different relaxation channels governing the green and violet luminescence.

The comparison of the PL spectra with the cathodoluminescence (CL) spectra of the same samples⁶ reveals differences in the relative intensity of the excited emissions. The 2.8 and 3.2 eV PL bands appear in the CL spectra as shoulders of a main broad green 2.4 eV emission band. However, for NiO samples annealed in vacuum both the 2.4 and 3.2 eV bands have a comparable spectral weight and clearly visible multippeak structure. The green 2.4 eV band is visible in time-resolved PL spectra recorded at 10 K for different delay times⁶. At variance with Ref. 8 the PL and CL emission bands observed in this work⁶ were attributed to the crystal field d - d transitions.

To the best of our knowledge the photoexcitation of PL has been restricted by $E_{exc} = 4.43$ eV⁶ with no inspection of the PL photoexcitation over the CT band, though such a study can be an instructive tool to elucidate the mechanism of the CT transitions and the spectral selectivity of the PL. It is worth noting that all the studies of the PL in NiO point to a special role of different defects and the surface induced local non-cubic distortions in photoemission enhancement and a remarkable inhomogeneous broadening of the PL bands. Indeed, a most effective absorption of photons with the energy $\hbar\omega \sim E_g$ occurs in a thin (10-20 nm) surface layer with more or less distorted symmetry and enhanced defect concentration. In other words, the UV photoexcitation cannot stimulate the bulk luminescence mirroring the fundamental material properties. These issues did motivate our studies of the photoluminescence spectra in NiO under high-energy excitation with making use of the both VUV and soft X-ray time-resolved PL excitation technique.

II. EXPERIMENTAL RESULTS

The PL measurements were made on the samples of NiO and several solid solutions $\text{Ni}_{1-x}\text{Zn}_x\text{O}$ ($x = 0.2, 0.3,$ and 0.6) with rock salt crystal structure. As starting material we have used the commercially available powder of NiO (99%; Prolabo) and ZnO (99.99%; Alfa Aesar) which has been pressed into pellets under pressure of about 1250 bar and placed into gold capsules. Quenching experiments at 7.7 GPa and 1000-1100 K have been performed using a toroid-type high-pressure apparatus. Details of experimental technique and calibration are described elsewhere¹¹. Electron microscopy analysis shows the samples to be dense poreless oxide ceramics with rock salt cubic structure and grain size of about 10-20 μm . The NiO and $\text{Ni}_{0.3}\text{Zn}_{0.7}\text{O}$ ceramic samples has been stired and pressed into cellulose to enhance the luminescence intensity. The PL spectra have been excited by the synchrotron radiation (SR) with 1 ns pulses run-

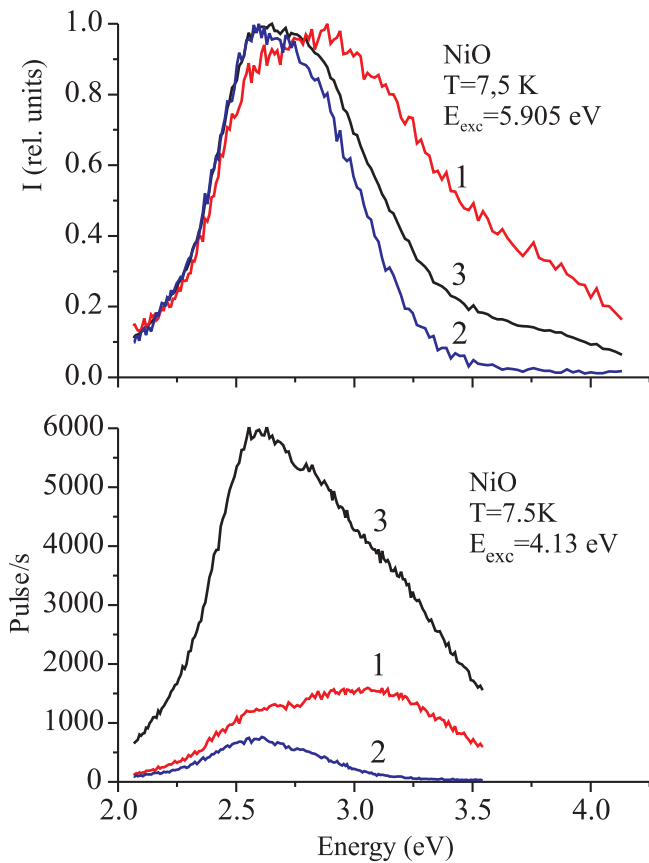


FIG. 2: (Color online) Time-resolved PL spectra (VUV - excitation) of NiO: 1 - fast window; 2 - slow window; 3 - time-integrated spectrum.

ning with 96 ns intervals. The PL and PLE spectra were recorded in 2-3.5 and 4-7 eV range, respectively¹². The measurements of PL spectra under soft X-ray (XUV) excitation were made on a SUPERLUMI station (HASYLAB (DESY), Hamburg) using an ARC Spectra Pro-308i monochromator and R6358P Hamamatsu photomultiplier. The time-resolved PL and PLE spectra, the PL decay kinetics in 1-80 ns interval were measured in two time windows: fast with a delay time $\delta t_1 = 0.6$ ns, span of windows $\Delta t_1 = 2.3$ ns; and slow delay time $\delta t_2 = 58$ ns, $\Delta t_2 = 14$ ns. The time-resolved PL spectra as well as the PL decay kinetics under XUV excitation has been measured on a BW3 beamline by a VUV monochromator (Seya-Namioka scheme) equipped with microchannel plate-photomultiplier (MCP 1645, Hamamatsu). The parameters of time windows: $\delta t = 0.1$ ns, $\Delta t = 5.7$ ns. The temporal resolution of the whole detection system was 250 ps. The temporary interval between SR excitation pulses is equal 96 ns.

Photoluminescence spectra of NiO under VUV-excitation at two energies $\hbar\omega > E_g$ and different registration regimes are presented in Fig. 2. The PL spectra have a complicated form depending on registration time and excitation energy. Time-integrated spectrum (Fig. 2,

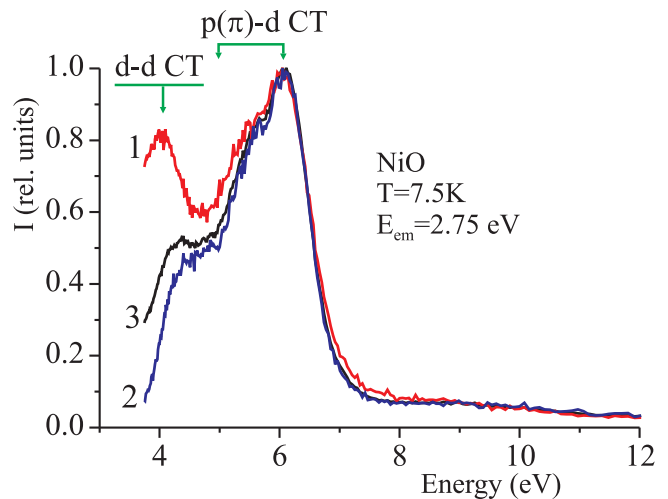


FIG. 3: (Color online) Time-resolved PLE spectra of NiO: 1 - fast window; 2 - slow window; 3 - time-integrated spectrum. Arrows point to $d(e_g)-d(e_g)$ and $p(\pi)-d$ ($t_{2u}(\pi) \rightarrow e_g$ and $t_{1u}(\pi) \rightarrow e_g$) CT transitions which are most effective in the luminescence excitation.

curve 3) has a maximum near 2.6 eV and an extended high-energy tail which is more intensive for the 4.13 eV than for the 5.9 eV excitation. Time-integrated spectrum at 4.13 eV excitation does correlate with the PL spectrum of NiO pressed powders observed in Ref. 6 at $T=10$ K and $E_{exc} = 4.43$ eV. A significant difference in PL spectra is revealed for fast and slow windows. High-energy 5.9 eV excitation results in a sizeable enhancement of PL in the high-energy range 3-4 eV for fast window, however, the 4.13 eV excitation gives rise to a more pronounced effect with the intensive maximum of the broad PL band shifted to 3.15 eV, while for slow window one observe a broad PL band peaked near 2.6 eV. It is worth noting that the PL spectrum for fast window and 4.13 eV excitation correlates rather well with that in Ref. 8 ($E_{exc} = 3.81$ eV, $T=10$ K). The PL excitation spectrum shown in Fig. 3 reveals a significant effect of different observation conditions. Time-integrated spectrum and the spectrum for slow window present a broad maximum near 6 eV and a shoulder near 4.5 eV. For fast window the shoulder transforms into a narrow peak near 4 eV comparable in magnitude with strong maximum near 6 eV.

It should be emphasized that the CT transition peaked near 4 eV working only in the fast window is the most effective in excitation of the high-energy (violet) part of the PL spectrum. Interestingly, the PLE spectrum correlates both with the reflectance¹³, electroreflectance¹⁴, and RIXS¹⁵ spectra of NiO in the region 4-6 eV. The PL decay kinetics is shown in Fig. 4 for $E_{exc}=4.13$ eV and different emission energies. The decay curves were approximated by a sum of two exponentials and a pedestal which describes a slow microsecond decay: $I(t) = y_0 + y_1 \exp(-t/\tau_1) + y_2 \exp(-t/\tau_2)$, where $\tau_1 = 3.4$ ns, $\tau_2 = 14.6$ ns, $y_0 = 0.11$ ($E_{exc} = 4.13$ eV, $E_{em} = 2.8$ eV); $\tau_1 = 2.3$ ns, $\tau_2 = 7.2$ ns,

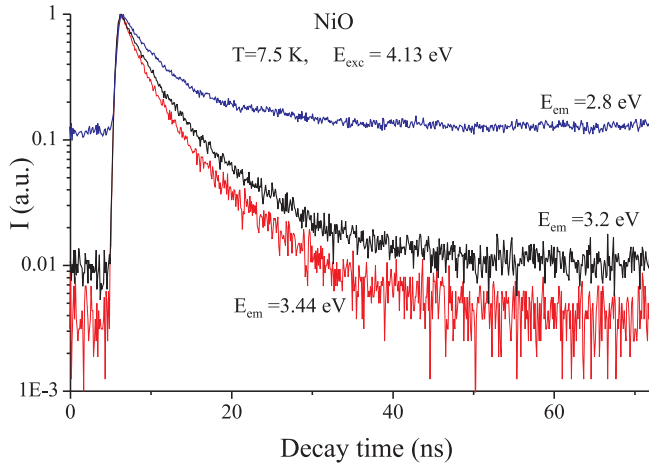


FIG. 4: (Color online) PL decay kinetics (VUV - excitation) of NiO.

$y_0 = 0.003$ ($E_{exc} = 4.13$ eV, $E_{em} = 3.44$ eV); $\tau_1 = 2.3$ ns, $\tau_2 = 16.7$ ns, $y_0 = 0.006$ ($E_{exc} = 5.9$ eV, $E_{em} = 2.8$ eV). Thus, time-resolved PL and PLE spectra, as well as the PL decay kinetics point to two relaxation processes in NiO with a characteristic times of nanoseconds and ten of nanosecond, respectively. Part of energy is emitted in micro- or millisecond range.

Luminescence spectra of NiO under XUV excitation with energy $E_{exc} = 130$ eV and fast window opening by 100 ps after the excitation impulse start are presented in Fig. 5. The XUV excited luminescence reveals puzzling spectral features with two close and very narrow lines I_1 and I_2 with a short decay-time $\tau < 400$ ps peaked for NiO sample at 3.310 eV (linewidth 17 meV) and 3.369 eV (linewidth 13 meV), respectively, mounted on a weak broad structureless pedestal in the 2.5-4 eV range which is actually observed only for slow window. To the best of our knowledge, such an unusual luminescence has not been observed to date either in NiO or other 3d oxides. From the other hand, the well isolated I_1 - I_2 doublet in the XUV excited luminescence seems to be a close relative of the broad high-energy (violet) band in PL spectra peaked near 3.2 eV. Dramatic difference in violet luminescence spectra under XUV and VUV excitation can be explained if to account for different penetration depth of VUV and XUV quanta. XUV excitation stimulates the bulk luminescence mirroring the fundamental material properties while the UV photoexcitation stimulates thin surface layers which irregularities give rise to a strongly enhanced and inhomogeneously broadened luminescence. To examine the origin of the unconventional I_1 - I_2 doublet and make more reasonable suggestions about its nature we have made the measurements of the XUV excited luminescence for solid solution $\text{Ni}_{0.3}\text{Zn}_{0.7}\text{O}$. As in NiO we observed the I_1 - I_2 doublet actually with the same energies and close linewidths. However, the integral intensity of the I_1 - I_2 doublet in $\text{Ni}_{0.3}\text{Zn}_{0.7}\text{O}$ is appeared to be almost ten times weaker than in NiO that points to the

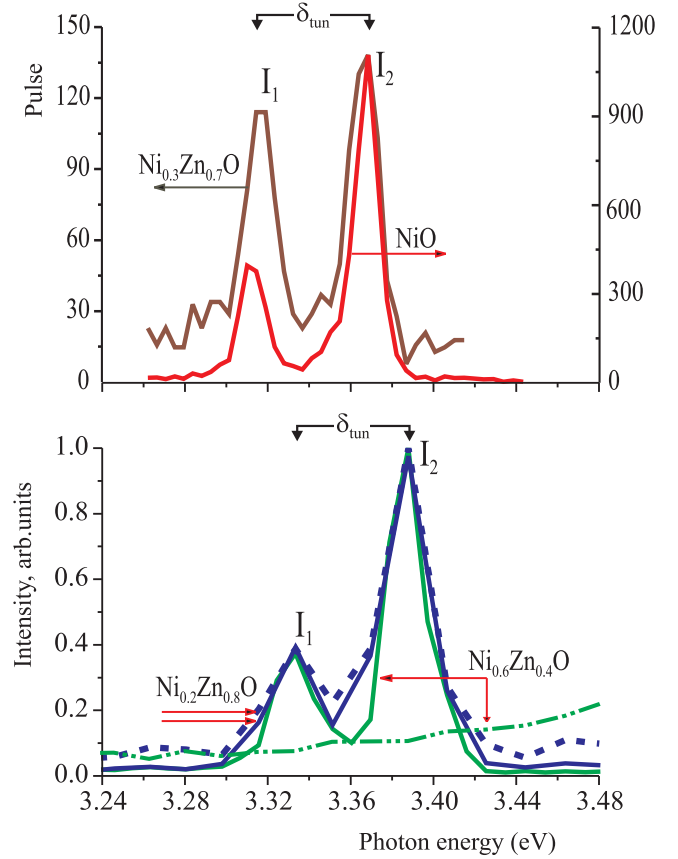


FIG. 5: (Color online) XUV excited luminescence spectra of NiO and solid solutions $\text{Ni}_x\text{Zn}_{1-x}\text{O}$ (fast window). Upper panel: Luminescence spectra of the cellulose coated NiO and $\text{Ni}_{0.3}\text{Zn}_{0.7}\text{O}$ samples under XUV excitation with energy $E_{exc} = 130$ eV at $T = 7.2$ K. Bottom panel: Low-temperature ($T = 7.5$ K) luminescence spectra of the $\text{Ni}_{0.2}\text{Zn}_{0.8}\text{O}$ and $\text{Ni}_{0.6}\text{Zn}_{0.4}\text{O}$ cellulose free samples under XUV excitation with energy $E_{exc} = 130$ eV (solid line) and $E_{exc} = 450$ eV (dashed line). Luminescence spectra of $\text{Ni}_{0.6}\text{Zn}_{0.4}\text{O}$ under XUV excitation with energy $E_{exc} = 130$ eV at $T = 7.2$ K (solid line) and room temperature (dash-and-dotted line).

relation of the I_1 - I_2 doublet with an emission produced by somehow coupled pairs of Ni ions. To exclude conceivable parasitic effect of the cellulose coating we have made the measurements of the XUV excited luminescence for cellulose free ceramic samples of solid solutions $\text{Ni}_{0.2}\text{Zn}_{0.8}\text{O}$ and $\text{Ni}_{0.6}\text{Zn}_{0.4}\text{O}$ (Fig. 5, bottom panel). For the both samples we have observed the same I_1 - I_2 doublet structure of the luminescence spectra with practically the same energy separation $\delta \approx 60$ meV and a small 20 meV blue shift as compared with NiO and $\text{Ni}_{0.3}\text{Zn}_{0.7}\text{O}$ samples. Such a shift is believed to arise from small strains induced by coatings. Interestingly, the novel luminescence is clearly visible only at low temperatures: room temperature measurements do not reveal noticeable effect (see RT spectrum for $\text{Ni}_{0.6}\text{Zn}_{0.4}\text{O}$ in Fig. 5 typical for other samples). As it is seen in Fig. 5 (bottom panel) the

XUV excitation with higher energy $E_{exc} = 450\text{ eV}$ does induce nearly the same I_1 - I_2 doublet structure of the luminescence spectra.

III. DISCUSSION

Charge carriers and excitons photogenerated in a crystal with strong electron-lattice interaction are known to relax to self-trapped states causing local lattice deformation and forming luminescence centers. Despite the nature of radiative and nonradiative transitions in strongly correlated $3d$ oxides is far from full understanding some reliable semiquantitative predictions can be made in frames of a simple cluster approach (see, e.g. Refs.16 and references therein). The method provides a clear physical picture of the complex electronic structure and the energy spectrum, as well as the possibility of a quantitative modelling. In a certain sense the cluster calculations might provide a better description of the overall electronic structure of insulating $3d$ oxides than the band structure calculations, mainly due to a better account for correlation effects. Starting with octahedral NiO_6 complex with the point symmetry group O_h we deal with five Ni $3d$ and eighteen oxygen O $2p$ atomic orbitals forming both hybrid Ni $3d$ -O $2p$ bonding and antibonding e_g and t_{2g} molecular orbitals (MO), and purely oxygen nonbonding $a_{1g}(\sigma)$, $t_{1g}(\pi)$, $t_{1u}(\sigma)$, $t_{1u}(\pi)$, $t_{2u}(\pi)$ orbitals. Ground state of $[\text{NiO}_6]^{10-}$ cluster, or nominally Ni^{2+} ion corresponds to $t_{2g}^6 e_g^2$ configuration with the Hund $^3A_{2g}$ ground term.

Typically for the octahedral MeO_6 clusters,¹⁶ the nonbonding $t_{1g}(\pi)$ oxygen orbital has the highest energy and forms the first electron removal oxygen state while other nonbonding oxygen π -orbitals, $t_{2u}(\pi)$, $t_{1u}(\pi)$, and σ -orbital $t_{1u}(\sigma)$ have lower energy with the energy separation $\sim 1\text{ eV}$ in between (see Fig. 1).

The p - d CT transition in NiO_6^{10-} center is related with the transfer of O $2p$ electron to the partially filled $3de_g$ -subshell with formation on the Ni-site of the $(t_{2g}^6 e_g^3)$ configuration of nominal Ni^+ ion isoelectronic to the well-known Jahn-Teller Cu^{2+} ion. Yet actually instead of a single p - d CT transition we arrive at a series of O $2p\gamma \rightarrow \text{Ni } 3de_g$ CT transitions forming a complex p - d CT band. It should be noted that each single electron transition gives rise to two many-electron transitions. The band starts with the dipole-forbidden $t_{1g}(\pi) \rightarrow e_g$, or $^3A_{2g} \rightarrow ^3T_{1g}, ^3T_{2g}$ transitions, then includes two formally dipole-allowed so-called $\pi \rightarrow \sigma$ p - d CT transitions, weak $t_{2u}(\pi) \rightarrow e_g$, and relatively strong $t_{1u}(\pi) \rightarrow e_g$ CT transitions, respectively, each giving rise to $^3A_{2g} \rightarrow ^3T_{1u}, ^3T_{2u}$ transitions. Finally main p - d CT band is ended by the strongest dipole-allowed $\sigma \rightarrow \sigma$ $t_{1u}(\sigma) \rightarrow e_g$ ($^3A_{2g} \rightarrow ^3T_{1u}, ^3T_{2u}$) CT transition. Above estimates predict the separation between partial p - d bands to be $\sim 1\text{ eV}$. Thus, if the most intensive CT band with a maximum around 7 eV observed in RIXS spectra^{4,15} to attribute to the strongest dipole-allowed O $2pt_{1u}(\sigma) \rightarrow$

Ni $3de_g$ CT transition then one should expect the low-energy p - d CT counterparts with maxima around 4 , 5 , and 6 eV respectively, which are related to dipole-forbidden $t_{1g}(\pi) \rightarrow e_g$, weak dipole-allowed $t_{2u}(\pi) \rightarrow e_g$, and relatively strong dipole-allowed $t_{1u}(\pi) \rightarrow e_g$ CT transitions, respectively (see Fig. 1). It is worth noting that the $\pi \rightarrow \sigma$ p - d CT $t_{1u}(\pi) \rightarrow e_g$ transition borrows a portion of intensity from the strongest dipole-allowed $\sigma \rightarrow \sigma$ $t_{1u}(\sigma) \rightarrow e_g$ CT transition because the $t_{1u}(\pi)$ and $t_{1u}(\sigma)$ states of the same symmetry are partly hybridized due to p-p covalency and overlap. Interestingly that this assignment finds a strong support in the reflectance (4.9 , 6.1 , and 7.2 eV for allowed p - d CT transitions)¹³ and, particularly, in electroreflectance spectra^{13,14} which detect dipole-forbidden transitions. Indeed, the spectra clearly point to a forbidden transition peaked near 3.7 eV (missed in reflectance spectra) which thus defines a p - d character of the optical CT gap and can be related with the on-set transition for the whole complex p - d CT band. It should be noted that a peak near 3.8 eV has been observed in nonlinear absorption spectra of NiO ¹⁸. A rather strong $p(\pi)$ - d CT band peaked at 6.3 eV is clearly visible in the absorption spectra of MgO:Ni ¹⁷.

As a result of the p - d CT transition, a photo-generated electron localizes on a Ni^{2+} ion forming Jahn-Teller $3d^9$, or Ni^{1+} configuration, while a photo-generated hole can move more or less itinerantly in the O $2p$ valence band determining the hole-like photoconductivity³. It is worth noting that any oxygen π -holes have larger effective mass than σ -holes, that results in the substantially distinct role of $p(\pi)$ - d and $p(\sigma)$ - d CT transitions both in photoconductivity¹⁹ and the luminescence stimulation.

The most effective channel of the recombinational relaxation for the spin-triplet p - d CT states $t_{2g}^6 e_g^3 \underline{\gamma}(\pi)$ ($\gamma(\pi) = t_{1g}(\pi), t_{2u}(\pi), t_{1u}(\pi)$) implies the $\pi \rightarrow \pi$ transfer $t_{2g} \rightarrow \gamma(\pi)$ with formation of excited spin-triplet $^3T_{1g}$ or $^3T_{2g}$ states of the $t_{2g}^5 e_g^3$ configuration of Ni^{2+} ion followed by final relaxation to lowest singlet terms $^1T_{2g}$ and 1E_g producing green and red luminescence, respectively. Obviously, this relaxation is strongly enhanced by any symmetry breaking effects lifting or weakening the selection rules. It means the three $\pi \rightarrow \sigma$ p - d CT transitions $t_{1g}(\pi) \rightarrow e_g$, $t_{2u}(\pi) \rightarrow e_g$, and $t_{1u}(\pi) \rightarrow e_g$ are expected to effectively stimulate the green luminescence due to large effective mass of π -oxygen holes and a well-localized and long-lived character of the p - d excitation. On the other hand, the most intensive $\sigma \rightarrow \sigma$ p - d CT transition $t_{1u}(\sigma) \rightarrow e_g$ appears to be significantly less effective due to small effective mass of the σ -oxygen holes and relatively short lifetime of the respective unstable p - d CT state. It does explain the lack of the 7 eV peak in the PLE excitation spectra (Fig. 3).

Thus, the $p(\pi)$ - d CT transitions are believed to effectively stimulate the green luminescence of NiO , yet these cannot explain the origin of violet luminescence, in particular, specific I_1 - I_2 doublet stimulated by XUV excitation which concentration behavior points to participation of Ni pairs, or d - d CT transitions rather than isolated

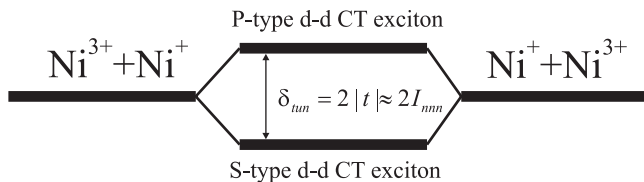


FIG. 6: Illustration to formation of S- and P-type $d-d$ CT excitons in NiO.

NiO₆ centers. Indeed, strong $d-d$ CT, or Mott transitions provide an important contribution to the optical response of strongly correlated 3d oxides¹⁶. In NiO one expects a strong $d-d$ CT transition related with the $\sigma - \sigma$ -type $e_g - e_g$ charge transfer $t_{2g}^6 e_g^2 + t_{2g}^6 e_g^2 \rightarrow t_{2g}^6 e_g^3 + t_{2g}^6 e_g^1$ between nnn Ni sites with the creation of electron [NiO₆]¹¹⁻ and hole [NiO₆]⁹⁻ centers (electron-hole dimer), or nominally Ni⁺ and Ni³⁺ ions. This unique anti-Jahn-Teller transition ${}^3A_{2g} + {}^3A_{2g} \rightarrow {}^2E_g + {}^2E_g$ creates a $d-d$ CT exciton self-trapped in the lattice due to electron-hole attraction and strong "double" Jahn-Teller effect for the both electron and hole centers. Exchange tunnel reaction $\text{Ni}^+ + \text{Ni}^{3+} \leftrightarrow \text{Ni}^{3+} + \text{Ni}^+$ due a two-electron transfer gives rise to two symmetric (S- and P-) excitons (see Fig. 6) having s- and p-symmetry, respectively, with energy separation $\delta = \delta_{tun} = 2|t|$, where t is the two-electron transfer integral which magnitude is of the order of Ni²⁺-Ni²⁺ exchange integral²⁰. Interestingly that P-exciton is dipole-allowed while S-exciton is dipole-forbidden.

Strong dipole-allowed Franck-Condon $d(e_g)-d(e_g)$ CT transition in NiO manifests itself as a strong spectral feature near 4eV clearly visible by the RIXS spectra (4.5eV)^{4,15}, the reflectance spectra (4.3eV)¹³, the non-linear absorption spectra (4.1-4.3eV)¹⁸, and, particularly, in our PLE spectra (4.1eV, see Fig. 3). Such a strong absorption near 4eV is beyond the predictions of the $p-d$ CT model and indeed is lacking in absorption spectra of MgO:Ni¹⁷. Accordingly, the CT gap in NiO is believed to be formed by a superposition of the electro-dipole forbidden $p-d$ ($t_{1g}(\pi) \rightarrow e_g$) and allowed $d(e_g)-d(e_g)$ CT transitions with close energies. The energy of the S-P doublet of the self-trapped $d-d$ CT exciton is expected to be $\sim 1.0-1.5$ eV lower than the energy of the $d(e_g)-d(e_g)$ peak, that is near 3eV, if to account for typical estimates for electron-hole attraction (~ 0.5 eV) and Jahn-Teller stabilization energy (~ 0.5 eV/one E-type state). It is worth noting that different optical reflectance and absorption measurements^{10,13,21} did not reveal the I_1-I_2 doublet.

Obviously the recombination of the self-trapped $d-d$ CT exciton, or, strictly speaking, of the S-P doublet

can explain all the features observed in the XUV excited luminescence spectra (Fig. 5). Weak line I_1 can be attributed to recombination of the dipole-forbidden S-exciton, while strong line I_2 with that for dipole-allowed P-exciton. The S-P separation ($\delta_{tun} \approx 60$ meV) agrees with theoretically predicted $\delta_{tun} \approx 2|I_{nnn}| \sim 70$ meV, if to make use of estimates for I_{nnn} in Ref. 2. Finally, the $d-d$, or pair character of this luminescence does explain its strong nonlinear suppression in solid solution Ni_{0.3}Zn_{0.7}O. It is worth noting that self-trapped $d-d$ excitons can be formed due to a trapping of the oxygen hole borned by the $p-d$ CT transition on the nearest Ni²⁺ ion.

IV. CONCLUSION

In summary, the luminescence spectra of NiO under VUV and XUV excitation have been investigated. PL spectra show broad emission bands centered at about 2.3 and 3.2 eV. The PLE spectra recorded in the 4-7 eV range agree with the RIXS and reflectance data. The PL spectral evolution and lifetime measurements under VUV excitation reveal that two mechanisms with long and short decay times, respectively, are responsible for the observed emissions. These mechanisms are related to $p(\pi)-d$ and $d(e_g)-d(e_g)$ CT transitions in the range 4-6 eV, while the most intensive $p(\sigma)-d$ CT transition at 7 eV appears to be a weak if any PL excitation mechanism. The $d(e_g)-d(e_g)$ CT transition peaked near 4 eV and working only in the fast window is the most effective one in the excitation of the high-energy (violet) part of the PL spectrum. For the first time we succeeded to distinctly separate contributions of $p(\pi)-d$, $p(\sigma)-d$, and $d-d$ CT transitions.

Making use of the XUV excitation allows us to avoid the predominant role of the surface effects in luminescence and reveal bulk luminescence with puzzling well isolated I_1-I_2 doublet of very narrow lines with close energies near 3.3 eV in both NiO and solid solutions Ni_xZn_{1-x}O. Comparative analysis of the $p-d$ and $d-d$ CT transitions, their relaxation channels, and luminescence spectra for NiO and Ni_{0.3}Zn_{0.7}O points to recombination transition in self-trapped nnn Ni⁺-Ni³⁺ $d-d$ CT excitons as the only candidate source of unconventional luminescence. To the best of our knowledge it is the first observation of the self-trapping for $d-d$ CT excitons.

The authors are grateful to R.V. Pisarev, V.I. Anisimov, and A.V. Lukoyanov for discussions and Dr. M. Kirm for help in BW3-experiments. This work was partially supported by the Russian Federal Agency on Science and Innovation (Grant No. 02.740.11.0217) and RFBR Grant No. 10-02-96032.

¹ Junbo Wu, Ce-Wen Nan, Yuanhua Lin, and Yuan Deng, Phys. Rev. Lett. **89**, 217601 (2002); Hisashi Shima, Fumiyoshi Takano, Hiro Akinaga, Yukio Tamai, Isao H. In-

oue, and Hide Takagi, Appl. Phys. Lett. **91**, 012901 (2007); H. Ohldag, A. Scholl, F. Nolting, E. Arenholz, S. Maat, A.T. Young, M. Carey, and J. Stöhr, Phys. Rev. Lett. **91**,

- 017203 (2003).
- ² B. Brandow, Adv. Phys. **26**, 651 (1977); S. Hüfner, Adv. Phys. **43**, 183 (1994).
 - ³ Ja.M. Ksendzov and I.A. Drabkin, Sov. Phys. Solid State, **7**, 1519 (1965).
 - ⁴ N. Hiraoka, H. Okamura, H. Ishii, I. Jarrige, K.D. Tsuei, and Y.Q. Cai, Eur. Phys. J. B **157-162** (2009).
 - ⁵ J. Zaanen, G.A. Sawatzky, and J.W. Allen, Phys. Rev. Lett. **55**, 418 (1985).
 - ⁶ C. Díaz-Guerra, A. Remón, J.A. García and J. Piqueras, Phys. Stat. Solidi (a), **163**, 497 (1997).
 - ⁷ V.V. Volkov, Z.L. Wang, and B.S. Zou, Chemical Phys. Lett. **337**, 117 (2001).
 - ⁸ S. Mochizuki and T. Saito, Physica B, **404**, 4850 (2009).
 - ⁹ A. Kuzmin, N. Mironova-Ulmane and S. Rochin, Proceedings SPIE, **5122**, 61 (2003).
 - ¹⁰ R. Newman and R.M. Chrenko, Phys. Rev. **114**, 1507 (1959).
 - ¹¹ A.N. Baranov, P.S. Sokolov, O.O. Kurakevich, V.A. Tafeenko, D. Trots and V.L. Solozhenko, High Pressure Research, **28**, 515 (2008).
 - ¹² V.A. Pustovarov, V.Yu. Ivanov, V.I. Sokolov, N.B. Gruzdev, A.N. Baranov, P.S. Sokolov, DESY, HASY-LAB, Annual Report-2010, Hamburg, Germany, 20101113 (2011).
 - ¹³ R.J. Powell and W.E. Spicer, Phys. Rev. B **2**, 2182 (1970).
 - ¹⁴ J.L. McNatt, Phys. Rev. Lett. **23**, 915 (1969); R. Glosser, W.C. Walker, Solid State Commun, **9**, 1599 (1971).
 - ¹⁵ L.-C. Duda, T. Schmitt, M. Magnuson, J. Forsberg, A. Olsson, J. Nordgren, K. Okada and A. Kotani, Phys. Rev. Lett. **96**, 067402 (2006); B.C. Larson, Wei Ku, J.Z. Tischler, Chi-Cheng Lee, O.D. Restrepo, A.G. Eguluz, P. Zschack, and K.D. Finkelstein, Phys. Rev. Lett. **99**, 026401 (2007).
 - ¹⁶ A. S. Moskvin, Phys. Rev. B **65**, 205113 (2002); R.V. Pisarev, A.S. Moskvin, A.M. Kalashnikova, and Th. Rasing, Phys. Rev. B **79**, 235128 (2009); A.S. Moskvin, R.V. Pisarev, Low Temp. Phys. **36** 613 (2010); A. S. Moskvin, Optics and Spectroscopy, **111**, 403 (2011).
 - ¹⁷ K.W. Blazey, Physica **89B**, 47 (1977).
 - ¹⁸ S.I. Shablaev, and R.V. Pisarev, Physics of the Solid State **45**, 1742 (2003).
 - ¹⁹ Most probably Ksendzov and Drabkin³ observed the $p(\pi)$ hole conductivity in a halide-decomposition NiO crystal stimulated by forbidden $p(\pi)$ - d ($t_{1g}(\pi) \rightarrow e_g$) CT transition, whereas an attempt to observe photoconductivity in flame-fusion-grown NiO crystals gave negative results up to 7 eV¹³, that is up to the energy of allowed $p(\sigma)$ - d ($t_{1g}(\sigma) \rightarrow e_g$) CT transition stimulating the $p(\sigma)$ hole conductivity.
 - ²⁰ A. S. Moskvin, Phys. Rev. B **84**, 075116 (2011).
 - ²¹ V. Propach, D. Reinen, H. Drenkhahn, H. Müller-Buschlaum, Z. Naturforsch., **33B**, 619 (1978).